VEHICLE ACCELERATION ESTIMATION USING SMARTPHONE-BASED SENSORS

F.J.BRUWER and M.J. BOOYSEN

Department of E&E Engineering, Stellenbosch University, Private Bag X1, Matieland, 7602
Tel: 021 808-4013; Email: mjbooysen@sun.ac.za

ABSTRACT

Recent advances in smartphone technology, including motion sensing and wireless communications, have resulted in these devices being used for vehicle-based driver behaviour sensing applications, replacing existing bespoke vehicle-based solutions. Acceleration is normally used as the primary indicator for recklessness. Despite the many benefits of using a smartphone to determine vehicle acceleration, the mobility of the phone relative to the vehicle, and the vehicle relative to the earth, causes the earth's gravitational force to obscure the true vehicle acceleration as perceived by the phone. The design and test results in this paper demonstrate how quaternions and an unscented Kalman filter can be used to remove the gravitational vector from the sensed acceleration, which enables reckless driving detection.

1 INTRODUCTION

One of the prevalent trends in the contemporary mobile industry is the use of the powerful integrated sensors in mobile devices to gather and process information on our everyday lives; a trend which branches from the biggest buzzword in modern electronics: *The Internet of Things*. These sensors have been put to good use by the safety industry to monitor the elderly for falls and accidents, but have yet to be properly implemented to monitor one of the most perilous parts of our everyday lives, namely commuting (WHO, (2010)). Gainwe et al. (2010), presents statistics showing that human error accounts for 86.4% of fatal crashes per year. The advent of smartphone-based sensing could provide a simple, inexpensive way to identify and reduce reckless driving.

The accelerometer features prominently in most proposed vehicle monitoring and reckless driving detection systems (Zeeman et al. (2014), Schietekat et al.(2013), Engelbrecht et al. (2014)) In vehicle monitoring, it is imperative to distinguish between accelerating, decelerating and lateral acceleration, since this data can be used to identify and classify driving manoeuvres and events effectively. Accurate coordinate acceleration data is therefore the main concern of this paper.

Accelerometers, however, measure what is known as proper acceleration (the acceleration relative to a free falling point), not coordinate acceleration (the acceleration relative to a stationary point). The proper acceleration of an object that is stationary with respect to the earth will therefore be 1 G (1 x 9.81m.s^{-2}) upwards in the earth axes.

Within a vehicle monitoring system, there are three sets of axes of concern: the earth axes, the vehicle axes and the sensor axes. The conventions for these axes are illustrated in Figure 1. In a dynamically moving vehicle with a smartphone-based sensor providing measurements, these axes are not necessarily constrained by known or fixed orientations

relative to one another. The accelerometer measurement in the sensor axes will therefore be corrupted by the effect of gravity with an unknown orientation.

The effect of gravity can be removed from the proper acceleration reading (in the sensor axes) if the orientation of the sensor axes relative to the earth axes can be found. The coordinate acceleration in the sensor axes can be rotated from the sensor axes to the vehicle axes if the orientation of the sensor relative to the vehicle can be determined; thereby yielding the coordinate acceleration in the vehicle axes.

The aim of this paper is to present a way of quantitatively measuring, recording and displaying the acceleration of a vehicle along its own axes, with the effect of gravity removed, to enable reckless driving detection. This is to be done using only the sensors commonly found in a smartphone (accelerometer, gyroscope, and magnetometer).

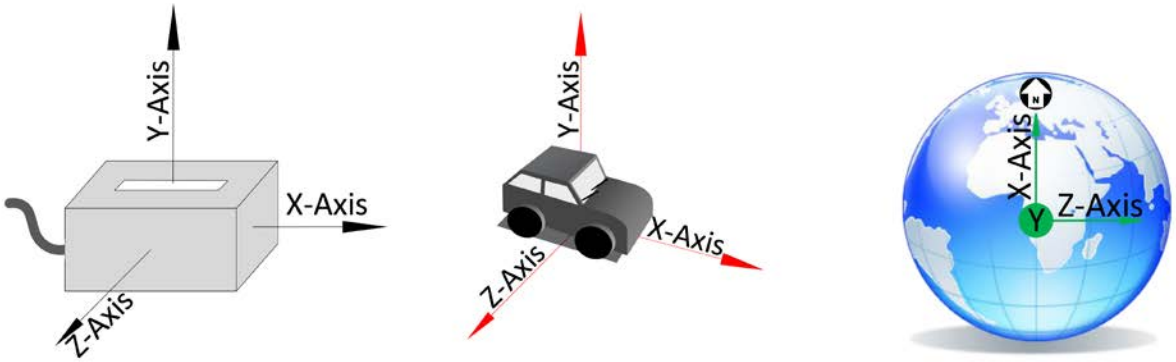

Figure 1 - Illustrations showing the conventions for the orientations of the sensor-, vehicle- and earth-axes respectively.

2 RELATED WORK

Many studies have been done on sensor attitude estimation using accelerometers, magnetometers and gyroscopes. The removal of gravitational acceleration from accelerometer data is also a common problem that has been well documented and researched.

Mizell (2003), attempted to ascertain whether it is possible to use an accelerometer placed at an arbitrary orientation on a body to infer reliable information on the movements of the body. The accelerometer reading was essentially high pass filtered to obtain the "dynamic" acceleration disregarding gravity and then rotated with vector operations so the moving average of the accelerometer reading (which is assumed to correspond to gravity) aligns with the vertical axis. The assumption that gravity corresponds to the long term average of the accelerometer reading is, however, inaccurate when working with a vehicle, body or sensor of which the orientation varies relative to gravity.

Xiaoping Yun et al. (2003), presented an improved quaternion-based Kalman filter for real-time tracking of a body's orientation. This is done using Magnetometer, Accelerometer and Gyroscopic sensors (MARG) and a standard Kalman filter. To allow the use of the standard Kalman filter, a linear relationship between states as well as additive noise is assumed. For quaternion orientations and angular rates, however, the assumption that noise is additive is incorrect and the quaternion rotation that takes place between states is non-linear. Furthermore, no attempt is made to take into account known system dynamics when transitioning between states.

Kraft (2003), similarly presents a method for real-time tracking using MARG sensors, but an unscented Kalman filter (UKF) is used, allowing a non-linear state-transition function and non-additive noise. Measurements from all three sensors are passed directly to the UKF, therefore a non-linear relationship exists between the observation and the state. This creates a very computationally demanding program. No attempt is made to use the orientation data to remove gravity from the acceleration measurement.

Jung Keun Leeet al. (2012), recognized the need for a combined implementation of attitude and coordinate acceleration estimation. This is done using a gyroscope and a magnetometer as well as an adapted Kalman filter algorithm. All calculations were done using rotation matrices which are computationally less efficient than quaternions. Furthermore, the system was not adapted for specific vehicle dynamics and no attempt was made to translate the axes of the final data to a body other than that of the sensor, which is necessary for sensing using a mobile device.

It is clear that, despite much research in the field of orientation estimation no system has been proposed where, accelerometer, magnetometer, gyroscope and vehicle dynamics information is used to efficiently estimate the coordinate acceleration of a vehicle using a mobile device placed within the vehicle.

3 DESIGN

For this paper, the use of a smartphone and smartphone-based sensors was emulated by using a sensor hub (gyroscope, accelerometer and magnetometer) connected via USB to a mobile computer running the software based estimator.
The basic operation of the software based estimator can be summarised as follows:

1. The system is initialised while the vehicle is stationary.
2. As the vehicle accelerates for the first time after start-up, the orientation of the vehicle relative to the sensor is calculated.
3. The orientation of the sensor relative to earth is calculated
4. The known gravitational acceleration is rotated from the earth axes to the sensor axes.
5. The gravitational acceleration in the sensor axes is then subtracted from the current acceleration measurement in the sensor axes.
6. The resulting gravity free acceleration is then rotated from the sensor axes to the vehicle axes.

Steps 3 to 6 are repeated to update the acceleration estimation.

These steps are discussed in more detail in the following sections and Figure 3 illustrates the flow of data within the system.

3.1 Calibration

The sensors are assumed to be stationary for the first 200 cycles of the program (4-8 seconds, processor dependent). A progress bar indicates the progress of calibration. During this time and continuing until the sensors are detected to be moving (accelerating), a moving average and variance of 200 samples is calculated by using two First In First Out (FIFO) queues and two 9-dimensional variables containing the sum of the data in the queues.
For the accelerometer reading, this moving average is used as an estimate of the earth's gravity in the sensor axis. For the gyroscope reading, the mean is used as the constant gyroscope bias and is subtracted from the gyroscope data received. For the

magnetometer, this mean value is of no particular significance. The calibration for the magnetometer is done by subtracting the lowest value encountered from the reading and then dividing by the difference between the highest and the lowest value encountered. It is recommended that the highest and lowest values encountered be obtained by rotating the device through all its axes in the environment that it is expected to be used in. For this system, these high and low values are read from a calibration file at system start up, updated whenever the program is running and saved when the program exits successfully.

3.2 Calculating the orientation of the vehicle relative to the sensor

The calibration of sensors stop and the recording of the first acceleration starts when the device starts moving (accelerating). The transition from stationary to accelerating is, for this paper, defined by a sustained difference between acceleration magnitude and the mean of the acceleration up to that time. The difference must be greater than the standard deviation of the previous acceleration measurements multiplied by a predefined tolerance. The first acceleration is recorded by summing all sampled acceleration data for the first period that the device is moving and dividing the sum by the number of samples taken.
Orientation of the vehicle relative to the sensor is calculated using the direction of the first acceleration in the sensor axes, the direction of gravity in the sensor axes and the assumption that gravity lies in the vehicle's X-Y plane.

The objective is to find the quaternion describing the rotation from the sensor axes to the vehicle axes. An objective function which can be minimized to find the most accurate quaternion rotation q_S^V is shown in equation 1.

$$\boldsymbol{f}\left(\boldsymbol{q_S^V}, \boldsymbol{d^V}, \boldsymbol{m^S}\right) = \boldsymbol{q_S^V} \otimes \boldsymbol{d^V} \otimes \boldsymbol{q'^V_S} - \boldsymbol{m^S} \quad (1)$$

Where d^V represents the direction of the front of the vehicle in the vehicle axes and m^S is the normalized measurement of the first acceleration in the sensor axes.

$$d^V = 0 + 1i + 0j + 0k \quad (2)$$

$$m^S = 0 + m_x i + m_y j + m_z k \quad (3)$$

The objective function is minimized by using the gradient descent method. The gradient descent algorithm is a simple algorithm both to implement and compute. This iterative algorithm is described by equations 4 - 6 with the Jacobian (J) of the objective function $\boldsymbol{f}$:

$$x_+ = x_c - \mu \times \frac{\Delta f}{||\Delta f||} \quad (4)$$

$$\Delta f = J^T f \quad (5)$$

$$\mu_t = \alpha ||\dot{q}_S^E|| \Delta t \quad (6)$$

Here, μ_t is the step size, which is directly proportional to the gyroscope rate, this prevents overshooting at low rotational speeds and enables faster tracking at high rotational speed. The Jacobian matrix of the objective function in equation 1 was calculated mathematically.

The gradient descent algorithm is iterated over until the adjustment is less than 1×10^{-4}.

3.3 Calculate the orientation of sensor relative to earth:

To avoid local minima with the gradient descent algorithm, an informed guess is made as to the initial orientation of the sensor relative to earth. This is done by checking the stationary mean of the gravity vector to see if the acceleration is upwards (positive y-direction) or downwards (negative y-direction). If the acceleration (gravity) is negative in the y-axis, a quaternion with a $180°$ roll is defined as the initial guess, otherwise a zero-quaternion is used (no rotation).

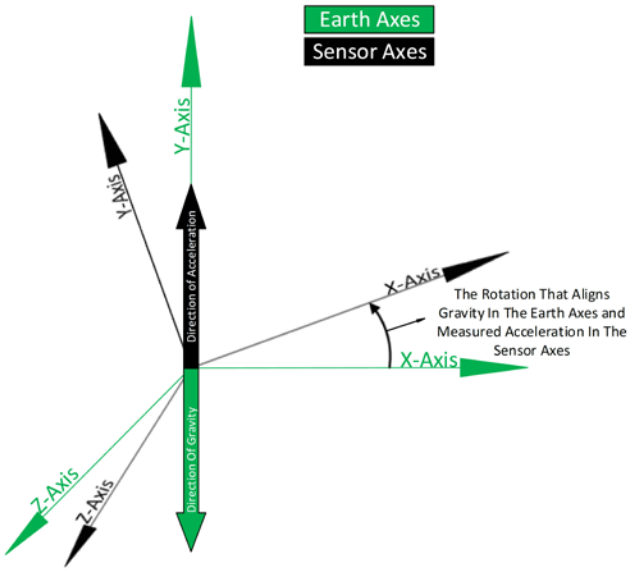

Figure 2 - An illustration of the rotation q_E^S and how it is estimated using an accelerometer reading.

3.3.1 Initialize Unscented Kalman filter:

An Unscented Kalman Filter (UKF) is used to combine accelerometer-, gyroscope-, magnetometer- and vehicle dynamics data in a way that maximises the probability of a correct estimation of the sensor's orientation relative to the earth axes.

The parameters needed to initialize an UKF are:

- Transition function. *f*
- Observation function. *g*
- Transition covariance. *Q*
- Observation covariance. *R*
- Initial state mean. μ_0
- Initial state covariance. Σ_0

The optimal state vector is chosen as the four part quaternion orientation with the three part rotational velocity appended as shown in equation 7.

$$x_k = [q_1, q_2, q_3, q_4, \omega_1, \omega_2, \omega_3]^T \quad (7)$$

A combination of the two objective functions similar to that in equation 1 (one for the accelerometer reading and the vertical y-axis and one for the magnetometer reading and

magnetic north) is minimized by using the gradient descent method described in equations 4 - 6.

For a live implementation such as the one in this paper, only one iteration of the gradient descent algorithm is needed per time step.

The resulting quaternion also contains a yaw-rotation from the magnetometer reading, this reading was found to have a delay relative to the other readings and was very inaccurate. The yaw of the vehicle around the earth's y-axis is of little significance when performing reckless driving detection and was therefore removed. This yaw-removal was done by converting the quaternion orientation (q_E^S) to Euler angles. These angles were then used to create a new quaternion using the same convention, but with the yaw-angle equal to zero. Figure 2 illustrates the rotation between the earth and sensor axes.

The 4-part quaternion orientation calculated here is combined with the 3-part gyroscope reading to provide an observation vector (shown in equation 8) for the UKF.

$$x_k = [q_{m1}, q_{m2}, q_{m3}, q_{m4}, \omega_{m1}, \omega_{m2}, \omega_{m3}]^T \quad (8)$$

3.3.2 Update Kalman filter:

For the first run, the Kalman filter is updated with the same mean and covariance used to initialise the filter as well as the observation vector defined in equation 8. For each successive iteration of the program the Kalman filter is updated with the mean and covariance output from the previous Kalman filter as well as the new observation vector.

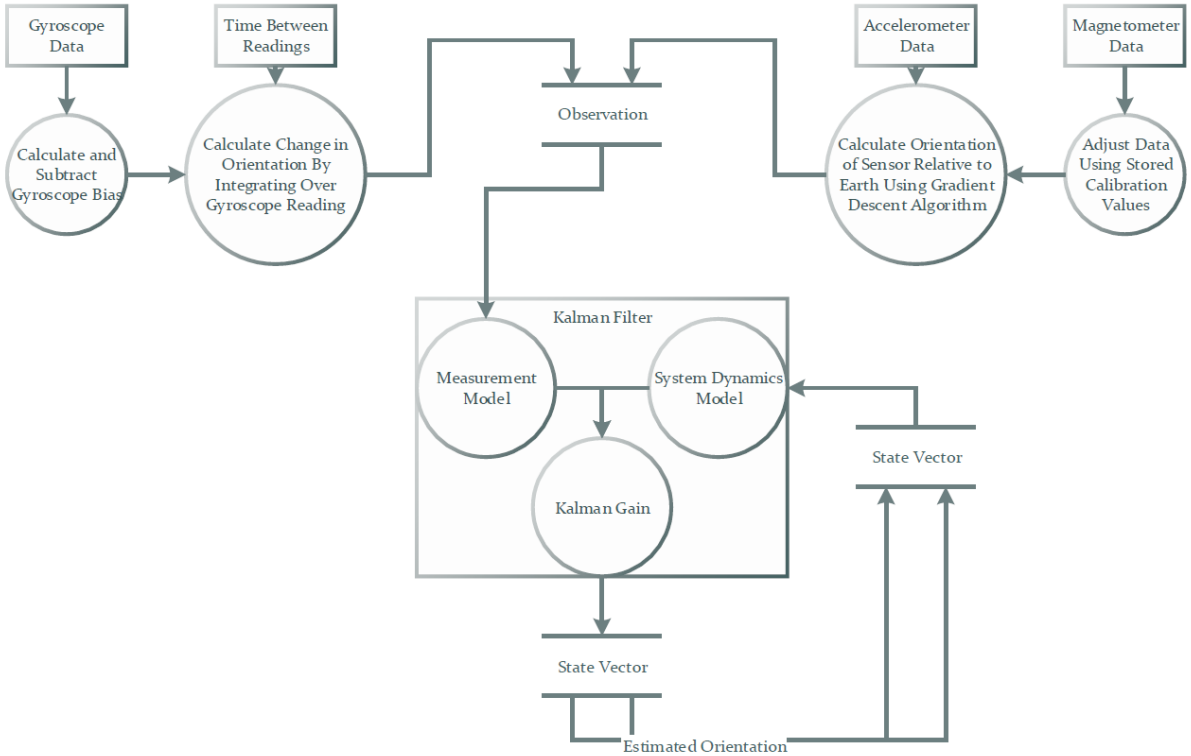

Figure 3 - A Data flow diagram illustrating the underlying flow of data within the system.

3.4 Rotate gravity from the earth- to the sensor axes:

At this point, all the necessary data to remove gravity from the accelerometer reading and to provide the absolute acceleration in the vehicle axes ($\overline{a^V}$) is available. This includes the

raw accelerometer data in the sensor axes (a^S), the gravity vector in the earth axes, the orientation of the vehicle relative to the sensor axes (q_S^V), and the orientation of the sensor relative to the earth axes (q_E^S). The magnitude of gravity in the earth axes can now be rotated into the sensor axes as shown in equation 9.

$$g^S = q_E^S \otimes g^E \otimes q'^S_E \qquad (9)$$

3.5 Remove gravity from acceleration measurement:

This gravitational acceleration in the sensor axes can now be subtracted from the sensor measurement as shown in equation 10.

$$\overline{a^S} = a^S - g^S \qquad (10)$$

3.6 Rotate resultant acceleration to vehicle axes:

The resulting acceleration in the sensor axes can now be rotated to the vehicle axes as shown in equation 11.

$$\overline{a^V} = q_S^V \otimes \overline{a^S} \otimes q'^V_S \qquad (11)$$

3.7 Record and visualise acceleration:

The resultant calculated acceleration data is visualised to better facilitate the comprehension of what has been achieved in this paper. The data is also recorded to enable the analytical measurement of the accuracy of the results.

At each iteration of the program, the resulting three axis acceleration in the vehicle axes as well as the time elapsed since the previous reading is written to a comma separated value (.csv) file for later use.

The data is displayed using Visual Python. A 3D set of axes that represent the earth's axes are displayed in green and a red object of which the orientation is easily identifiable, represents the vehicle's axes. The orientation of the red object is defined by a combination of the quaternions q_E^S and q_S^V as shown in equation 12.

$$q_E^V = q_E^S \otimes q_S^V \qquad (12)$$

The position of the red object relative to the origin represents the instantaneous acceleration of the vehicle in the vehicle axes. Examples of the 3D model's orientations and positions are shown in Figure 4.

The magnitude of the acceleration is also shown by the bars in Figure 5.

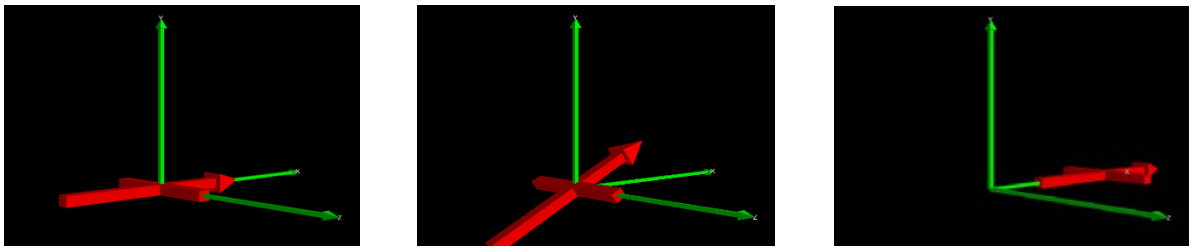

Figure 4 - The above screen shots show the position and orientation of the 3D model for situations where the vehicle is not accelerating, on an incline at constant speed, and accelerating on a level road respectively.

Figure 5 - A screen shot of the magnitude bars of the acceleration (lateral, vertical, and forward). The colours of the bars also vary from green, for small acceleration magnitudes, to red, for large acceleration magnitudes.

4 RESULTS

The testing of the system proved to be a non-trivial task, as a known acceleration with a constant known sensor orientation is difficult to reproduce. The novel tests that were implemented to thoroughly test the system and quantify errors are shown in Table 1.

Table 1- A table showing the various tests done and the motivations for doing them.

Test:	**Motivation:**
Stationary test	Used as a baseline and to quantify sensor noise.
Constant speed & level road test	To quantify the noise contributed by vehicle vibrations, road roughness and - irregularities at different speeds.
Deceleration test, no incline	To compare theoretical average x-axis deceleration over an interval with the average measurement over the interval.
Deceleration test on an incline	To test whether gravitational acceleration influences the measurements and if the vehicle-sensor orientation can be correctly calculated on an incline.
Constant speed & varying incline test	To test if the system can adjust for sudden changes in incline.
Constant speed & turn radius test	To test for accurate lateral acceleration data.

As the system is designed to be used in a vehicle, tests were done with the sensor in a secure position in the vehicle. For all tests, the normal calibration procedure is followed where the vehicle remains stationary on a road with a level horizontal gradient for the duration of calibration and is then accelerated forward in order for the system to determine the orientation of the sensor relative to the vehicle. All speeds are measured and saved programmatically with a GPS, as vehicle speedometers tend to be less accurate. All graph scales are chosen to correspond to the highest acceleration measured during vehicle testing.

Table 2 - A table showing the results of a deceleration test done on a constant incline.

		X	Y	Z
40km/h	Acceleration Duration (s)	2.761		
	Theoretical Avg. Acceleration (mG)	-410.22	0	0
	Acceleration RMS Error (mG)	12.91	21.58	5.10
	Error Magnitude (mG)	25.66		
60km/h	Acceleration Duration (s)	5.42		
	Theoretical Avg. Acceleration (mG)	-313.40	0	0
	Acceleration RMS Error (mG)	43.31	19.39	12.76
	Error Magnitude (mG)	49.14		

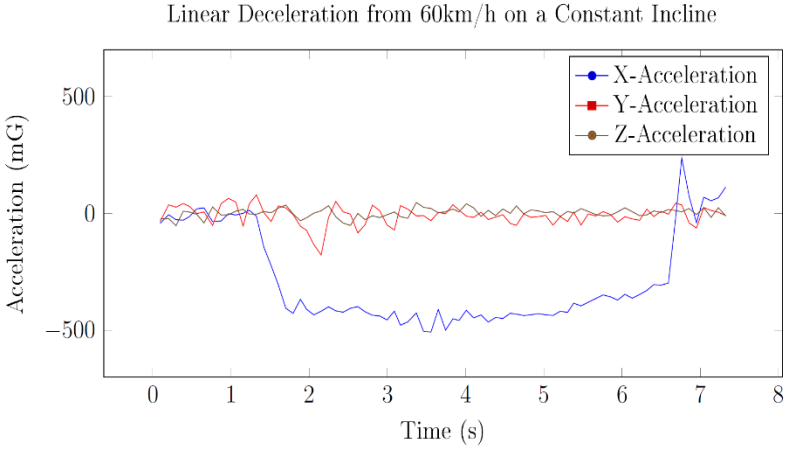

Figure 6 - A graph showing the acceleration data for a deceleration from 60km/h to stationary on a constant incline.

4.1 Discussion of results:

Comprehensive vehicle testing of the final system was done and the measured results were compared to theoretically calculated results as shown in Table 2. All results appeared to be accurate when compared to theoretical values and indicated good system operation, except for the sustained lateral acceleration test. The minimal acceleration error in the vehicle x- and z-axis during constant speeds shows that acceleration events of 30 mG or more are detectable by the system. This opens doors for, not only reckless driving detection, but applications where smaller accelerations are of concern, such as road quality detection, lane control and swerve detection, and efficient cruise-control algorithms. The vehicle's x-axis acceleration does not notably change due to changes in incline, indicating that the effect of gravity is effectively eliminated and that the resulting acceleration represents a accurate coordinate acceleration and not a proper acceleration. The acceleration tests also indicated that the vehicle's x-, y- and z-axis acceleration data vary independently, proving that that the resulting acceleration data is rotated accurately to the vehicle axes. Figure 6 shows graphically the independent variation of the x-axis acceleration during a deceleration on a constant incline. One problem area was identified. The assumption that the effect of a vehicles yaw with respect to north on reckless driving detection is negligible adversely affected the operation of the Kalman Filter.

It is therefore clear that, except for prolonged lateral accelerations, the system is accurate and would be beneficial for a reckless driving detection system.

5 CONCLUSION

The goal of this paper was to remove the effects of gravitation vector from the acceleration measured by a smartphone in a vehicle. This was done to enable detection of reckless driving behaviour, which is primarily based on vehicle acceleration. The objective was met by using the gyroscope, magnetometer, and acceleration sensors with an unscented Kalman filter and quaternions to estimate the gravitation acceleration. The estimated gravitation vector is then removed from the acceleration vector measured by the smartphone, to determine vehicle acceleration. The results show that the system enables accurate measurement of reckless events in various conditions. A Video Demonstration of detector in action in a vehicle can be found at: https://youtu.be/c3QpE-namqw.

6 REFERENCES

Engelbrecht, J., Booysen, M.J. and van Rooyen, G.J., (2014). Recognition of Driving Manoeuvres using Smartphone-Based Inertial and GPS Measurement. Paper presented at Proceedings of the first International Conference on the use of Mobile Informations and Communication Technology (ICT) in Africa UMICTA. STIAS Conference Centre, Stellenbosch: Stellenbosch University, Department of Electrical & Electronic Engineering, South Africa. 9-10 December 2014.

Gainewe, M. & Masangu, N., 2010. *Factors leading to fatal crashes and fatalities on the south african roads:2005-2009.* Pretoria, s.n.
World Health Organization, 2010. *Global Status Report on Road Safety,* Geneva: s.n.

Jung Keun Lee, Park, E.J. & Robinovitch, S.N. (2012)., Estimation of Attitude and External Acceleration using Inertial Sensor Measurement during various Dynamic Conditions. Instrumentation and Measurement, IEEE Transactions on, 61(8).

Kraft, E.. (2003). A Quaternion-Based Unscented Kalman Filter for Orientation Tracking. Paper presented at Proceedings of the Sixth International Conference of Information Fusion.

Mizell, D.. (2003). Using Gravity to Estimate Accelerometer Orientation. Paper presented at Wearable Computers, 2003. Proceedings. Seventh IEEE International Symposium on.

Schietekat, J.M. and Booysen, M.J.. (2013). Detection of Reckless Driving in the Sub-Saharan Informal Public Transportation System using Acceleration-Sensing Telematics. Paper presented at EUROCON, 2013 IEEE.
World Health Organization, (2010). *Global Status Report on Road Safety,* Geneva: s.n.

Xiaoping Yun, Lizarraga, M., Bachmann, E.R. and McGhee, R.B., (2003). An Improved Quaternion-Based Kalman Filter for Real-Time Tracking of Rigid Body Orientation. Paper presented at Intelligent Robots and Systems, 2003. (IROS 2003). Proceedings. 2003 IEEE/RSJ International Conference.

Zeeman, A. S. & Booysen, M. J., (2014). Public transport sector driver behaviour: Measuring recklessness using speed and acceleration paper delivered at the 33rd annual Southern African Transport Conference, CSIR International Convention Centre Pretoria, South Africa on 7 - 10 July 2014.